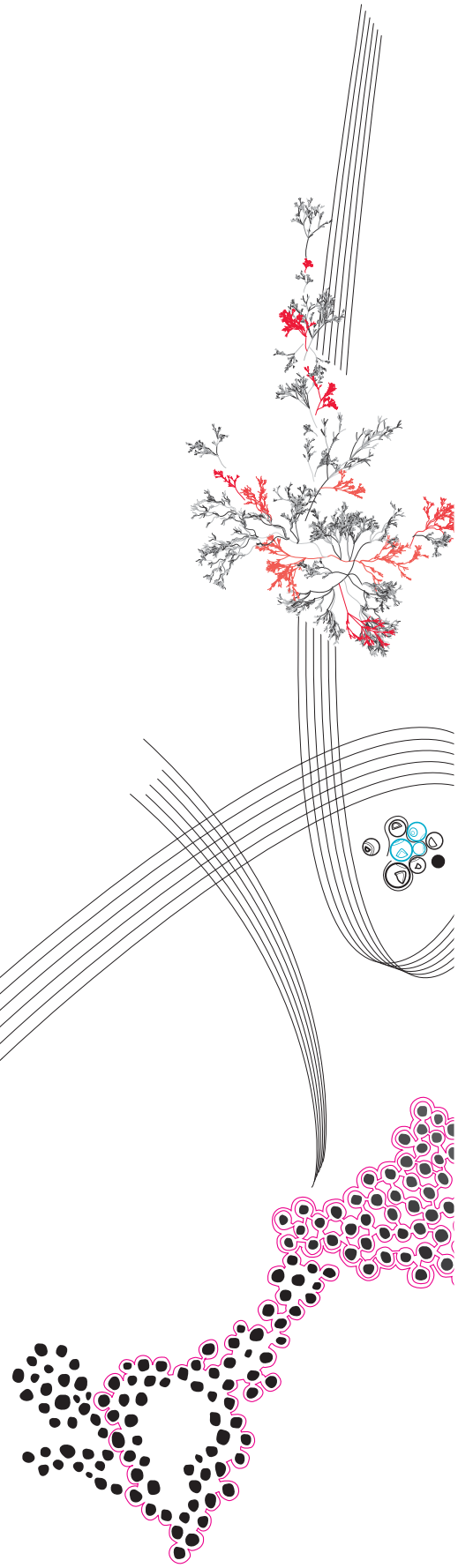

BSc Thesis Biomedical Technology

Laser Doppler Flowmetry, using in vitro phantoms to study skin microcirculation

Michiel van Lookeren Campagne

Supervisor: prof.dr.ir. Wiendelt Steenbergen
Daily supervisor: dr.ir. Ata Chizari
External committee member: ir. Hadi Mirgolbabaee

May , 2023

Department Science & Technology

UNIVERSITY OF TWENTE.

Laser Doppler Flowmetry, using in vitro phantoms to study skin microcirculation.

Michiel. J.A. van Lookeren Campagne

May , 2023

Abstract

Laser Doppler flowmetry (LDF) is a technique to measure perfusion in the skin. It uses the optical Doppler effect to measure the movement of bl
This research has taken a first step towards understanding the composition of laser Doppler flowmetry signals. In vivo LDF measurements were performed to gain experience with the system and to observe differences in the signal. The measurements showed a unique cardiac pattern in the perfusion signal. SDF was done to visualise the microcirculation of blood within the skin.
As a first step in the simulation of microcirculation, phantoms were made with a 100 µm diameter channel. To examine the shape of the channels in the phantoms, brightfield and fluorescence microscopy has been performed. Then, a blood flow was realised inside the channels. An LDPM measurement was performed on this blood flow. Although a signal was obtained, no relationship between flow rate and perfusion could be established. In order to enable a comparison between the in vitro and in vivo measurements, systematic measurements should be carried out where the flow rate in the channel can be both controlled and optically measured.

Keywords: Laser-Doppler flowmetry, perfusion imaging, perfusion monitoring, sidestream darkfield microscopy, fluorescence microscopy, brightfield microscopy, microchannel, capillary, blood flow

Contents

1 Introduction

Laser Doppler flowmetry (LDF) is a technique for measuring blood flow in the microcirculation of the skin. It uses the optical Doppler effect to measure the movement of red blood cells (RBCs). The microcirculation in the skin consists of blood vessels with a diameter of less than 150 µm.

The overall aim of this research is to extract more information from laser Doppler flowmetry (LDF) and photoplethysmography (PPG) signals. These techniques use the absorption and scattering of blood in the skin to measure blood flow. The problem with both techniques is that they can only describe flow in arbitrary units. As a result, they provide little information about blood pressure and cardiac output.

This research focuses on understanding the technique and application of laser Doppler flowmetry. It uses the optical Doppler effect to measure the perfusion of the microcirculation in the skin. To find differences in the signal and to gain experience with the system, several LDF measurements will be taken on different parts of the body. Ideally, we would like to establish a link between in vivo and in vitro measurements.

Sidestream Darkfield Imaging [1] is used to further investigate the composition of the microcirculation. By illuminating with a colour that is mainly absorbed by red blood cells, blood vessels in the skin become visible.

To fully understand the composition of the microcirculation and the signal it produces, it is necessary to make phantoms with a channel in the micrometre range. Zakian and Dickinson [2] have shown that it is possible to make accurate LDF measurements on the millimetre scale. Research by Jonasson et al [3] shows that measuring an LDF signal on 150 µm diameter tubes is possible. Shams Kazmi at al [4] have used laser speckle contrast analysis to estimate the average velocity of RBCs in a microfluidic channel.

This research hopes to answer the following question: Can we measure a laser Doppler flowmetry signal on a micrometer-scale phantom? In what condition can we compare such measurements with in vivo measurements?

2 Theoretical background

2.1 Principles of Laser Doppler Flowmetry

Laser Doppler Flowmetry [5] is a technique for measuring blood flow in tissue. It uses the optical Doppler effect [6]. This effect occurs when light is scattered by a moving particle. When a scattering event occurs, the outgoing wave vector of the light changes. The frequency Doppler shift is equal to the dot product between the velocity of the moving particle and the variation between the incoming and outgoing wave vectors. The Doppler shift is defined by the equation 1. See figure 1 for an illustration of this phenomenon.

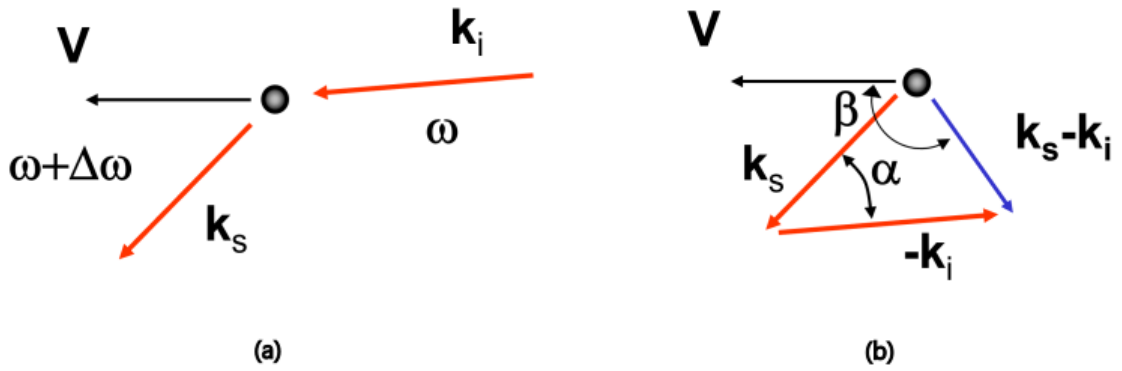

FIGURE 1: (a) shows a schematic representation of a Doppler scattering event. Figure (b) shows the difference in wave-vectors $K_s - K_i$ and the associated angles α and β.

$$\Delta\omega = V \cdot (K_s - K_i) = |V|\,|K_s - K_i| \cos\beta = \frac{4\pi}{\lambda}\,|V| \sin\frac{\alpha}{2}\cos\beta \tag{1}$$

where V is the velocity of the moving particle in m/s, K_i is the wave-vector of the incoming photon, K_s is the wave-vector of the scattered photon, λ is the wavelength of the light.

If you illuminate a sample containing moving scatterers with monochromatic light, some of the light will undergo a Doppler shift. Depending on the direction of movement, the frequency shift will be a positive or negative value. The result is a Doppler histogram. See figure 2. The graph shows the distribution of the photons versus their frequency. It is not possible to obtain this Doppler histogram in a real measurement.

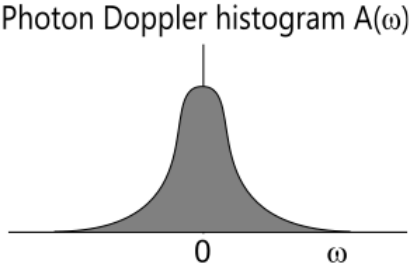

FIGURE 2: A photon Doppler histogram. The y-axis shows the amount of photons. The x-axis is the frequency domain

What is being measured is the photocurrent. This is the electrical signal from a photodiode. This signal changes as the intensity of the light reaching the detector changes. Due to the high frequency oscillations of light (a wavelength of 785 nm has a frequency of about 390 THz), the detector cannot measure this in real time. Typical (single) Doppler shifts are between 10 and 10000 Hz. This means that the change in frequency is very small. When two light waves of slightly different frequencies interfere, they form a wave that also oscillates at a frequency equal to the difference of their own frequencies (10 - 10000 Hz). This phenomenon is called an optical beat. See figure 3 for an illustration. Because these frequencies are relatively low, they can be detected by a photodiode.

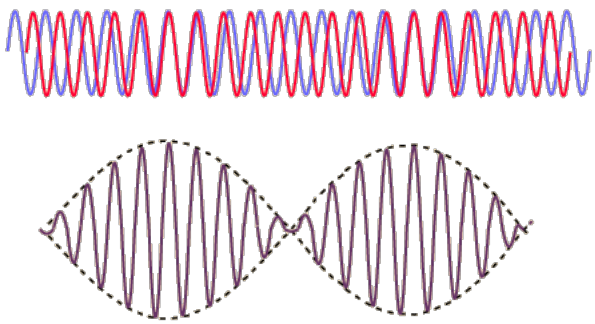

FIGURE 3: Schematic representation of the optical beat phenomenon. When two waves with different periods interact, the resulting wave has a period equal to the difference of the two waves. Image retrieved from: [7]

This intensity over time is measured by a photodetector. Taking the square of the Fourier transform of this (photocurrent) signal gives the power spectrum. The power spectrum gives the contribution of the different frequencies to the signal. See figure 4. For a proof of this connection, see: Fredriksson I et al, "Laser Doppler Flowmetry - a Theoretical Framework". [8].

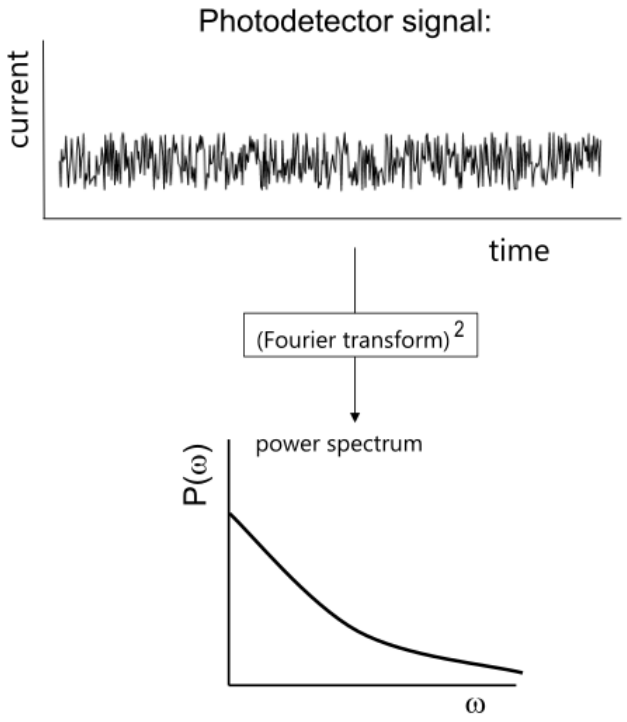

FIGURE 4: The power spectrum is obtained by squaring the Fourier transform of the photodetector signal.

The shape of the power spectrum depends on the concentration and movement of the RBCs. When the area under the power spectrum is integrated/summed, it is known to be proportional to the concentration of the RBCs. This is called the zeroth moment. See equation 2. Integrating the power spectrum multiplied by the frequency gives the first order moment. It is known that this is equal to the product between the concentration of RBCs and their average velocity. This product is called perfusion. But one of the limitations of laser Doppler flowmetry is that this signal is not quantitative yet. Therefore, this research will use arbitrary *perfusion units* [PU].

$$M_0 \equiv \int_0^\infty P(\omega)d\omega \propto C_s \qquad M_1 \equiv \int_0^\infty \omega P(\omega)d\omega \propto \underbrace{C_s \cdot V_s}_{\text{Perfusion}} \tag{2}$$

The penetration depth of laser Doppler flowmetry depends on factors such as laser power, wavelength and tissue anatomy. According to a study by Fredriksson et al. [9], this depth is between 0.5 and 1 mm. However, the constructed model only considers low power lasers on a small area. While this is true for the LDPM setup, the LDPI setup uses a high power laser and a large surface area. Therefore, the exact penetration depth is not known. However, it's assumed to be between 0.5 and 1 mm.

2.2 LDPI and LDPM

The laser Doppler signal can be measured in two ways. Either with a photodiode, where a photocurrent is measured over time. This means that measurements are made at a small point. This technique is called laser Doppler perfusion monitoring. See figure 5

(a). Another way to measure is to use a camera, where each pixel measures its own photocurrent. The result is a two-dimensional dynamic speckle pattern. See figure 5 (b) (For illustration purposes, the size of the speckles has been increased). The advantage of LDPI is that you can select your own region of interest in an image. The disadvantage is that it takes longer to process a measurement. LDPM is much faster and can be used for real-time measurements.

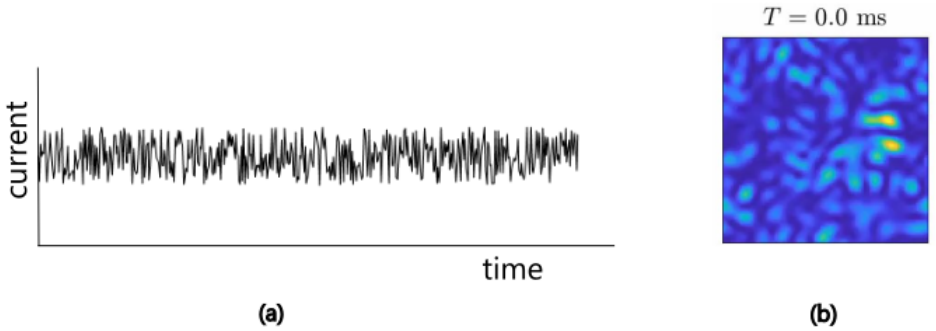

FIGURE 5: (a) A photocurrent over time, as measured by an LDPM device. (b) A two-dimensional speckle pattern, as observed by a LDPI setup (for illustration purposes, the speckle size is exaggerated).

2.3 Skin microcirculation

The LDF signal is a measure of the microcirculation in the skin. The microcirculation is roughly defined [10] as: blood vessels with a diameter of less than 150 µm. These are mainly arterioles, capillaries and venules. See figure 6.

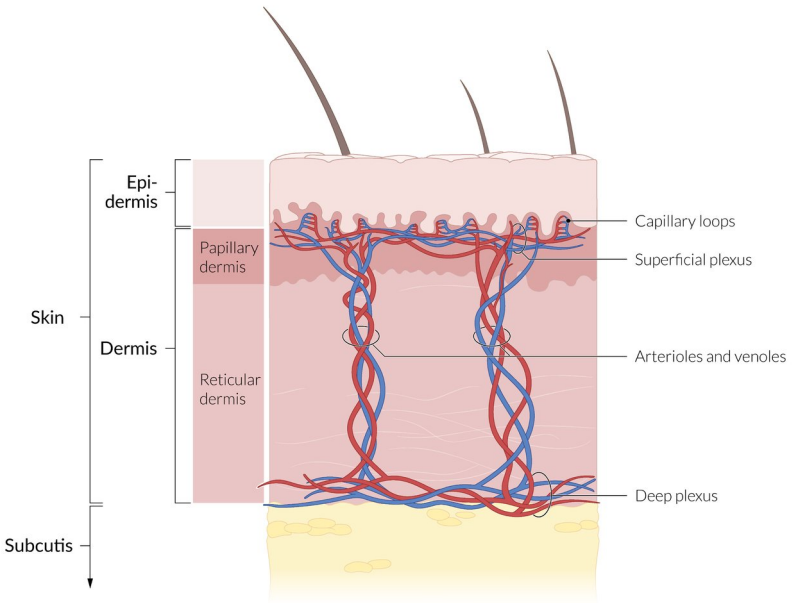

FIGURE 6: Schematic illustration of the blood vessels in the skin. The superficial and deep plexus are connected through arterioles and venules. Image retreived from: [11]

Human skin [12] varies in thickness from 1.5 to 4.0 millimetres or more, depending on the location on the body. It consists of two main layers. The *epidermis* forms the outermost protective layer of the body. It is composed entirely of epithelial cells and contains no blood vessels. It receives it's nutrients by diffusion from the lower layer.

Below the *epidermis* is the *dermis*. This makes up the bulk of the skin. It is a tough layer composed of connective tissue. It contains blood vessels, nerves, sweat glands, pores and hair roots.

The vascularisation of the dermis consists of two interconnected *plexi*; the superficial plexus and the deep plexus. The superficial plexus is located about 400-500 μm under the skin. It consists of capillaries through which diffusion takes place. These capillaries also form papillary loops through the dermal papillae. See figure 6. Arterioles and venules connect the superficial plexus to the deep plexus, which forms the boundary between the dermis and the fat layer.

2.4 Coupling pressure characterization

This research uses a setup where pipes of different diameters are connected together. When considering the flow through different tubes, it is useful to map the pressure characteristics using Bernoulli's equation (3).

$$P + \frac{\rho}{2}V^2 + \rho g h = \text{constant} \tag{3}$$

Where P is pressure in Pa, ρ is density in kg/m^3, V is flow velocity in m/s, g is the gravitational constant in m/s^2 and h is the height in m.

To use this equation, a few assumptions are made. First, that the fluid is Newtonian. Secondly, that it flows laminar, stationary and without resistance. It is not known what the resistance of our setup is, therefore this method is only used as an approximation.

$$P_1 - P_2 = \frac{\rho}{2}(V_2^2 - V_1^2) \tag{4}$$

The flow rate can be written as the flow rate divided by the cross sectional area:

$$V = \frac{Q}{A} \tag{5}$$

Where Q is the flow rate in m^3/s and A is the cross section in m^2. When the flow rate remains the same, the flow velocity depends on the cross sectional area. See equation 6.

$$V_2 = \frac{A_1}{A_2}V_1 \tag{6}$$

$$P_1 - P_2 = \frac{\rho}{2}V_1^2(\frac{A_1^2}{A_2^2} - 1) \tag{7}$$

When looking at this equation, there are a few things to consider. Firstly, the pressure difference increases with the square of the flow rate. Secondly, the pressure increases inversely to the square as the diameter of the second tube increases. When working with channels in the micrometre range, the pressure change increases rapidly. Especially when going from large to small diameters. It is therefore important to start with a low flow rate.

Figure 7 shows a plot of this pressure change. The inner diameters from the experiments were used to calculate the pressure change. The flow rate was set to 10 µl/min. Figure (a) shows the pressure change as a function of flow rate. (b) shows the pressure change as a function of the channel diameter.

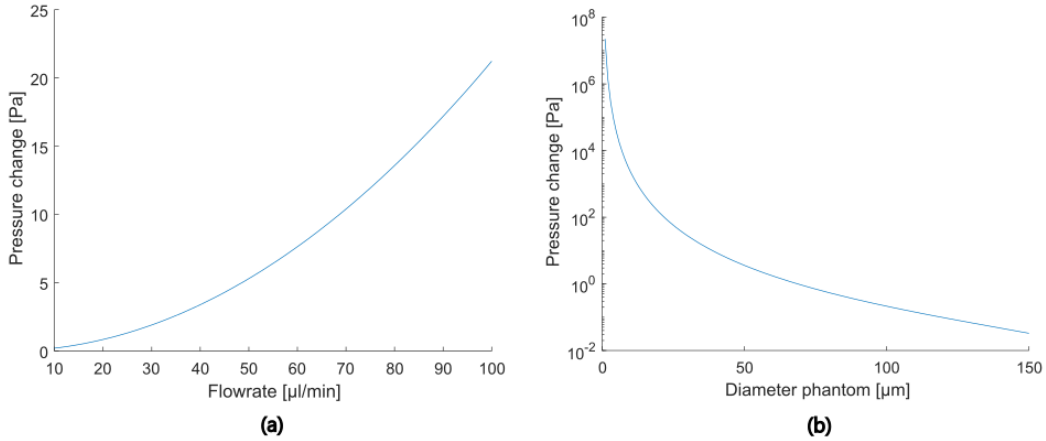

FIGURE 7: (a) the pressure change shown for variable flow rates, and channel diameter 100 µm. (b) the pressure change shown for variable channel diameter

2.5 Sidestream Darkfield Microscopy

To image the microcirculation of red blood cells in the skin, another imaging technique can be used. Sidestream darkfield microscopy [13] is a form of microscopy in which a single color of light is used to illuminate the specimen, rather than a broad spectrum of light (brightfield). By illuminating the sample from the side (sidestream), the reflected light can reach the detector through the centre (darkfield). See figure 8.

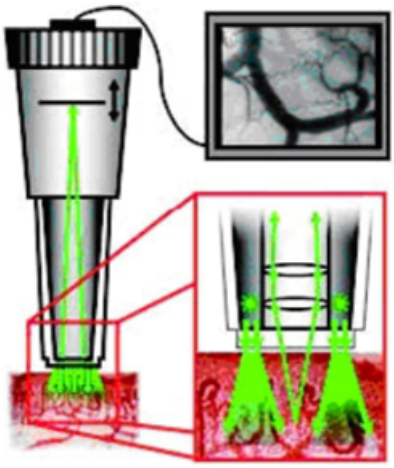

FIGURE 8: Schematic view of Sidestream Darkfield Imaging. A sample is illuminated by a ring of green LED's. The reflected light reaches the detector through the middle of the ring.

Some particles absorb more of this light than others. Higher absorption means less light is reflected. This produces an image where the high absorption spots are black and the low absorption spots are white. In human skin, a wavelength of 530 nm (green light) produces a high contrast image. This is because red blood cells have a high absorption at this wavelength, while the surrounding tissue does not. When looking at human skin, the red blood cells are black and all the other tissue is white. An example is shown at the top of the figure 8.

3 In Vivo: Materials and methods

3.1 In vivo LDPI measurements

3.1.1 Setup

The following setup was used to perform the LDPI measurements. Figure 9 (a) shows a picture of the setup. The flowchart in (b) shows the connections of each component in the setup. The detailed specifications of the components are given in the table 1.

Illumination is provided by a monochromatic laser (671 nm). The laser light is directed to the correct spot by two mirrors. Two lenses and an optical diffuser are used to give the laser the correct spot size. The reflected light is picked up by the camera through a series of components. A linear polariser is used to filter out most of the unshifted reflected light. The polariser is aligned to block out the maximum amount of reflected light. The light then passes through an optical bandpass filter. This allows only light around the wavelength of 675nm to pass. This is to block out any other light from other sources in the room. A lens is attached to the camera to focus the light onto the camera's detector, and the camera is connected to the PC via an Ethernet cable.

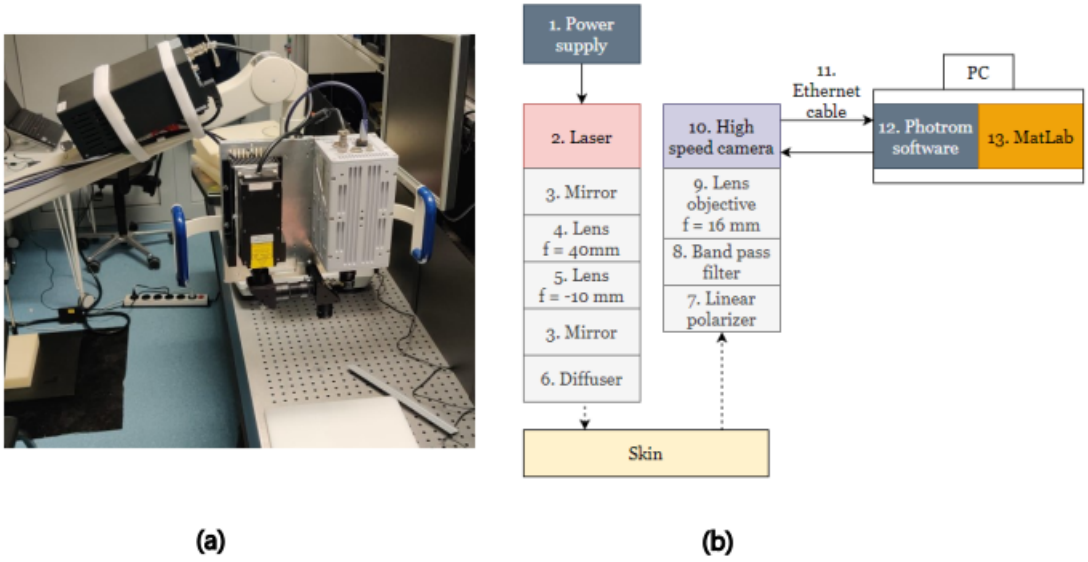

FIGURE 9: (a) A picture of the LDPI setup used during the experiments. (b) A Flowchart with all different components used in the setup. The exact details of each component is found in table 1.

Number	Specifications
1	CNI PSU-H-FDA. Input: 100-240VAC 5A
2	MSL-FN-671-300 mW
3	Thorlabs BB1-E02 mounted in KCB1C/M
4	Thorlabs LB1027-B f: 40 mm
5	Excelitas G052303322 f: -10 mm
6	Thorlabs ED1-C10-MD diffuser
7	Thorlabs LPNIRE100-B
8	Bandpass Filter 675 nm BW: 25 nm
9	Lens Kowa LM16HC f: 16 mm
10	Photron SA-3 Fastcam @ 25k FPS, 128 × 128 pixels
11	Gigabit ethernet cable
12	Photrom Fastcam Viewer 4.0.6.2
13	LDPI script

TABLE 1: A List of all the components from figure 9 (b), with their specifications.

3.1.2 Methods

The LDPI software uses a buffer length. During each buffer length (40 ms) the camera records 1000 data points. A power spectrum is generated from this signal. The first moment, see equation 2, is then calculated from the power spectrum. This first moment is one data point in the temporal perfusion signal. The buffer length is therefore a compromise between the accuracy of the power spectrum and the temporal resolution.

An LDPI measurement starts by calibrating (shading) the high-speed camera. This is done by covering the lens so that no light reaches the detector. The laser/camera arm is then aimed at the measurement spot at a distance of 40 cm. An area of 4.5 × 4.5 cm is

illuminated. All lights in the room are turned off to avoid adding noise to the signal. A button on the screen is then pressed to start the measurement. This is repeated for all the different measurements, as shown in the figure 10.

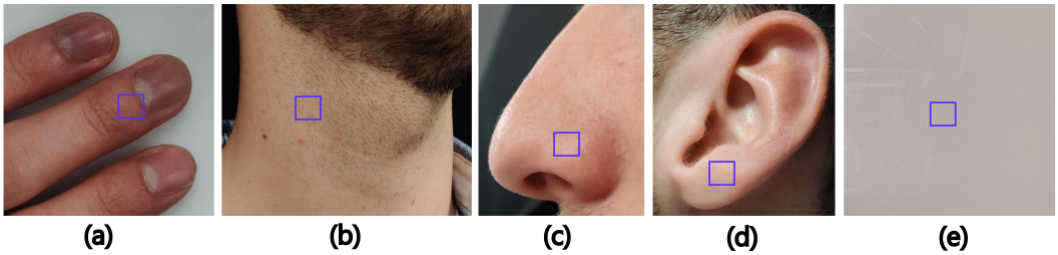

FIGURE 10: Images of spots that were measured in the experiment. (a) finger, (b) neck, (c) nose, (d) earlobe, (e) Delrin plate.

To analyze the data, a MatLab program is used (see figure 11. In this program, different parameters can be viewed and settings can be adjusted.

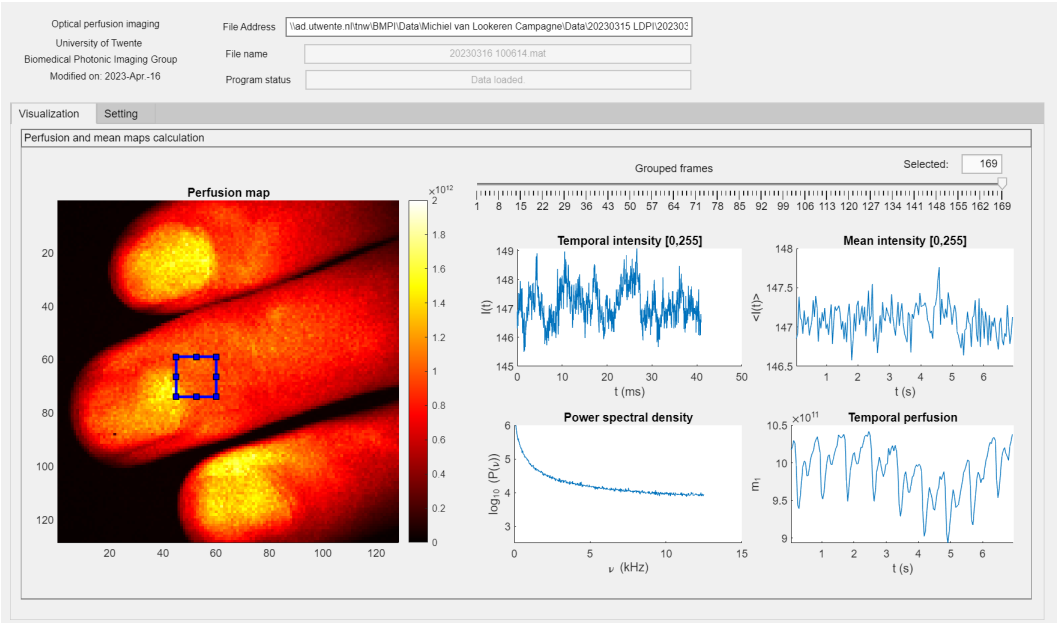

FIGURE 11: A screenshot of the MatLab program used to perform and analyze the LDPI measurements. The image on the left shows the perfusion of each pixel in the image. The blue square is the selected region of the interest. The figures on the right show the power spectrum, intensity and perfusion.

3.2 In vivo LDPM measurements

3.2.1 Setup

To perform the LDPM measurements, a Perimed Periflux 5000 device has been used. An optical probe is connected to the 5010 LDPM unit. This probe is placed into a circular probe holder. See figure 12.

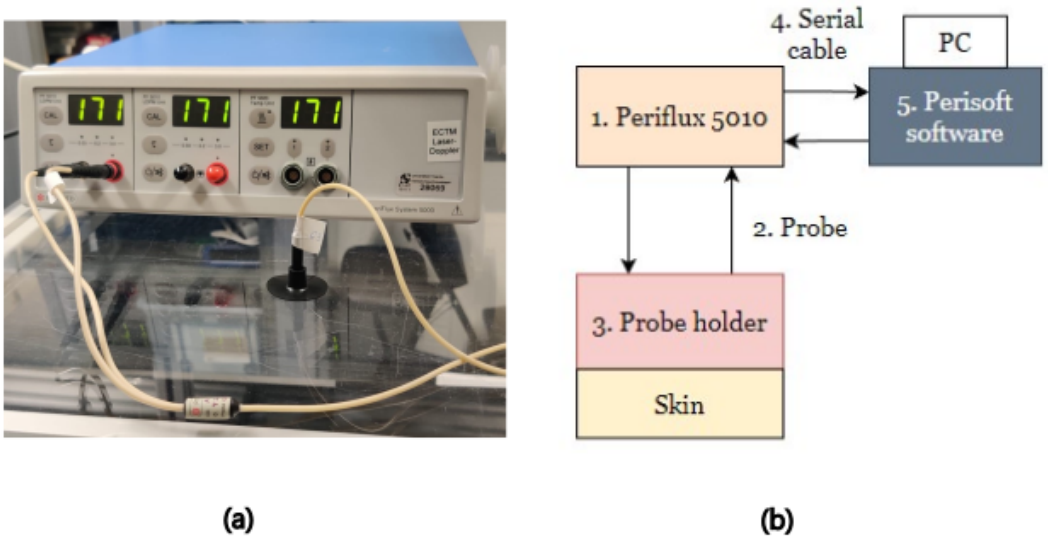

FIGURE 12: (a) The Perimed Periflux 5010 used in the experiments. (b) A schematic overview of the measurement setup.

Number	Specifications
1	Perimed Periflux 5010 LDPM system
2	Perimed 407-1 Probe. Fibre seperation 250 µm [14]
3	Circular probe holder. OD: 35 mm
4	PF490 serial cable
5	Perimed Perisoft 2.5.5

TABLE 2: The specifications of the components of the LDPM setup, as seen in figure 12 (b).

3.2.2 Methods

The Periflux LDPM device was allowed to warm up for twenty minutes before measurements were taken. The probe is placed in the circular probe holder to keep it perpendicular to the skin. A piece of double-sided tape is then placed on the probe holder to make it stick to the surface. The probe is then placed on the skin. The Perisoft software is used to start and stop a two minute measurement. These steps are repeated for the other spots as shown in the figure 10.

3.3 In vivo SDF microscopy

3.3.1 Setup

A Microvision Microscan was used to perform the SDF measurements. This device is placed directly on the skin. It is connected to a power supply which is then connected to a computer.

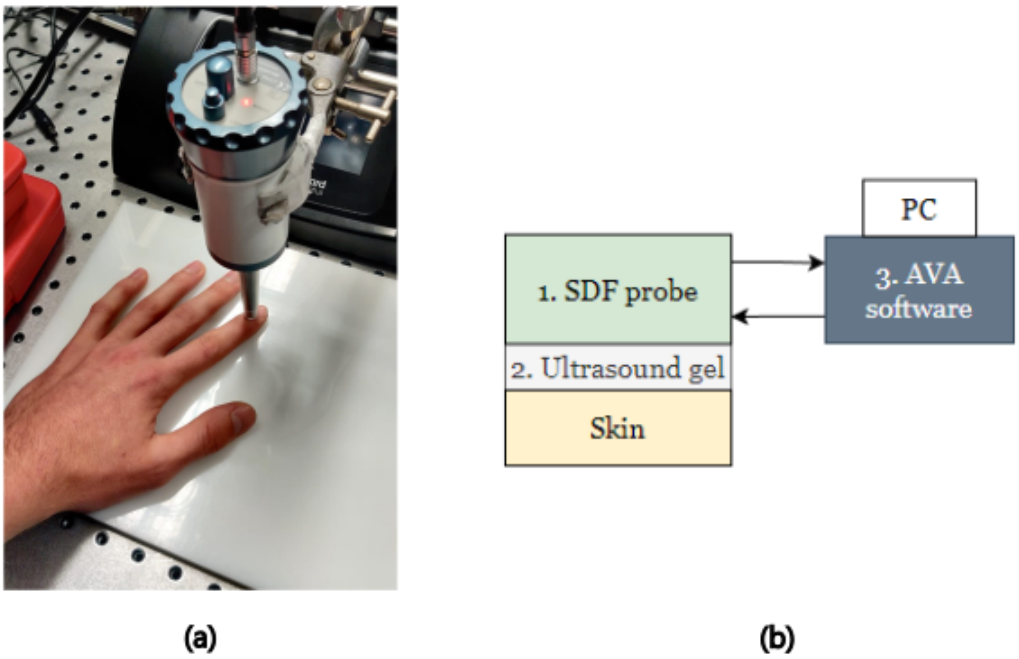

FIGURE 13: (a) The Microvision Microscan probe placed on the finger. (b) shows a schematic overview of the setup. The exact specifications can be found in table 3

Number	Specifications
1	Microvision Microscan
2	Sonogel electrodegel 3010
3	Automated Vascular Analysis

TABLE 3: The specifications of the components of the SDF setup, as seen in figure 13 (b).

3.3.2 Methods

Measurements were taken on the top of the finger, behind the nail. An image of this can be seen in figure 10 (a). First, a large drop of ultrasound gel is applied to the fingertip. The probe was then placed perpendicular to the finger. The data was received in the form of a video. This video was analysed with a script that improved the contrast with a narrow colour range.

4 In Vivo: Results

In this chapter, the results of the different experiments will be shown.

4.1 In Vivo LDPI measurements

Using the setup as described in 3.1.1 , measurements were done on five spots on the upper body. The results can be seen in the figure below.

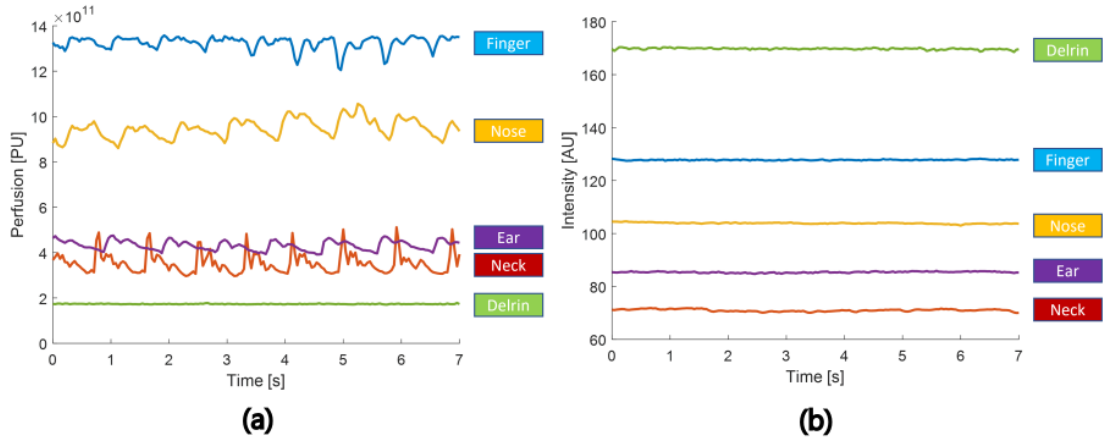

FIGURE 14: (a) shows the perfusion over time for each of the measurements. (b) shows the intensity over time. Videos of the measurements: 10.1 to 10.5.

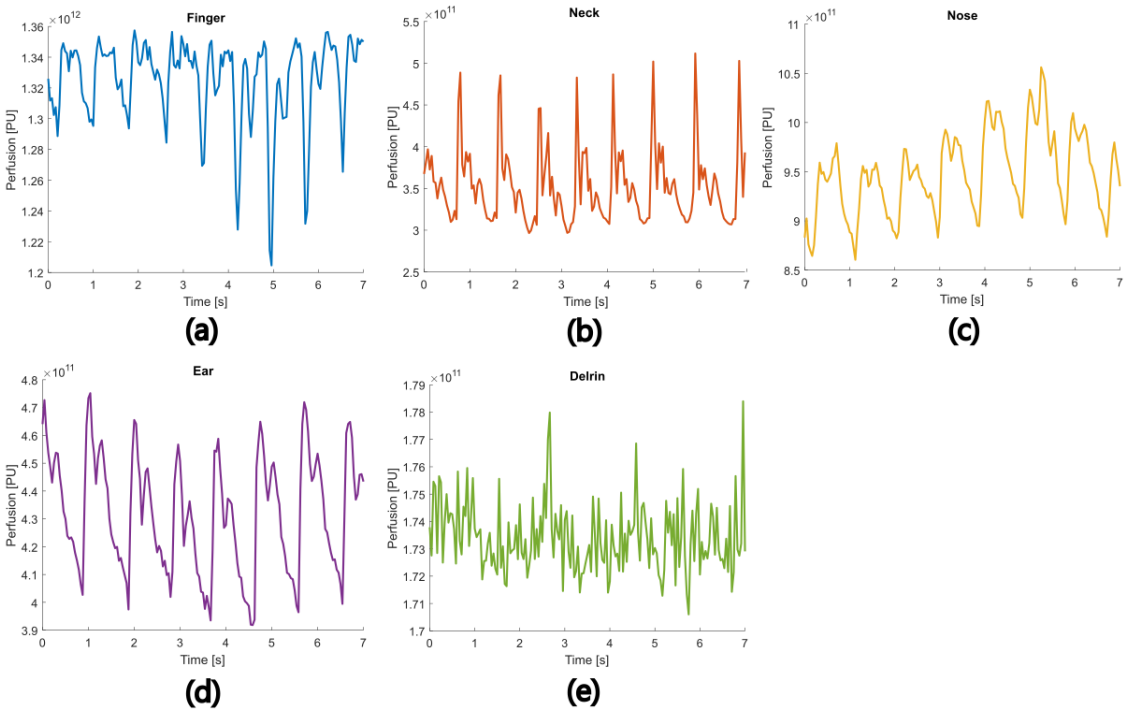

FIGURE 15: All the individual LDPI perfusion measurements. (a) finger, (b) neck, (c) nose, (d) ear, (e) Delrin plate.

4.1.1 Perfusion and intensity over time

As explained in 2, the perfusion is defined as the first moment of the power spectrum. The intensity of the signal is proportional to the photocurrent. See figure 5 (a).

In figure 14 (a) all perfusion signals can be seen relative to each other. Each different measurement shows a unique wave pattern. A clear cardiac cycle with a period of about one second is visible in all measurements. The finger and nose show the highest perfusion during the measurement. The ear and neck show relatively low perfusion. There's no big artefacts or noise visible. There's only a slight drift in the signal from the nose measurement. The control measurement on Delrin gives a constant but nonzero value. This is counter-intuitive, as there's no movement in a slab of Delrin.

Figure 14 (b) shows the intensity of each spot over time. All measurements show a very constant value. The Delrin plate clearly shows the highest intensity value. This is due to the large amount of reflected light reaching the camera, caused by the low absorption of the plate.

4.1.2 Power spectrum

The power spectrum tells us the contribution of different frequencies to the signal. Figure 16 shows two temporal LDPI measurements and their power spectra. (a) Shows the perfusion of an ear measurement. Two points are placed on the temporal plot. One point at a high perfusion value and another at a minimum value. In (b) the power spectra of these two points are shown. The spectra are quite similar up to a frequency of about 2000 Hz. The spectra then drift apart. In (c) the power spectra are multiplied by the frequency range. The integral of this line is how the first moment is calculated.

Figures (d), (e) and (f) show the Delrin measurement. There is no pattern or wave visible in the temporal perfusion signal. However, there is a difference in the power spectra at the lower frequencies. Up to a frequency of about 2000 Hz, the power of point 2 is higher. After 2000 Hz the spectra become very similar.

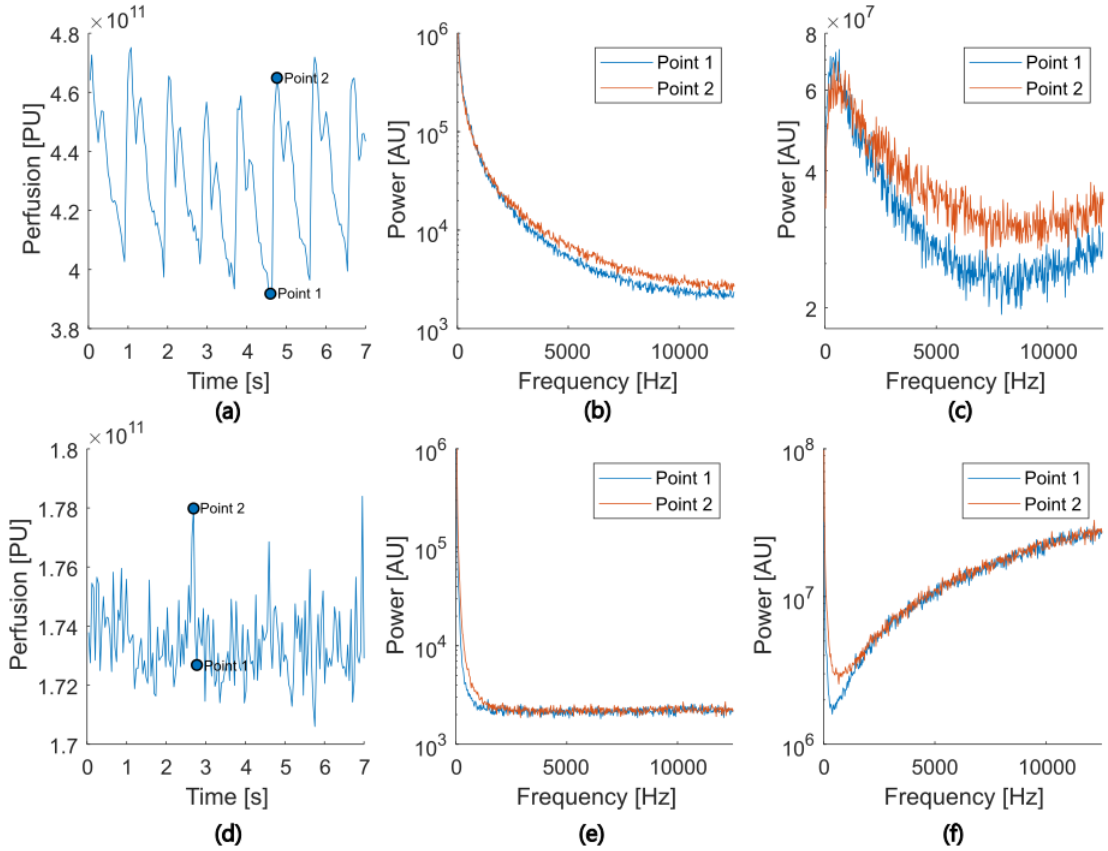

FIGURE 16: (a) Shows a temporal LDPI measurement on the ear. Two points during the measurement are marked. (b) shows the power spectra of these points. (c) First moment of the power spectrum. (d), (e) and (f) show the same for an LDPI measurement on a Delrin plate.

4.2 In vivo LDPM measurements

4.2.1 All measurements

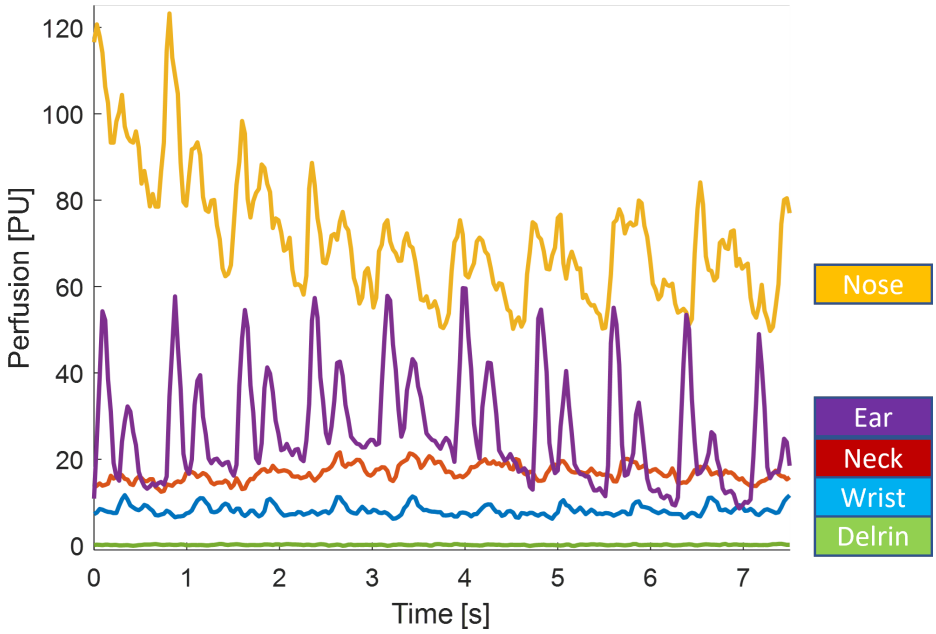

FIGURE 17: Each of the five LDPM measurements in one graph. The first seven seconds of each measurements is shown.

The spread of mean perfusion is less than with LDPI. The measurements contain a less clear heartbeat pattern and more noise. Especially the nose measurement. The clearest measurement is on the ear. Unlike all the others, there are two high peaks during each heartbeat. The neck gave no clear signal. The control measurement on the Delrin plate shows a constant value of almost zero. This shows that the instrument is correctly calibrated.

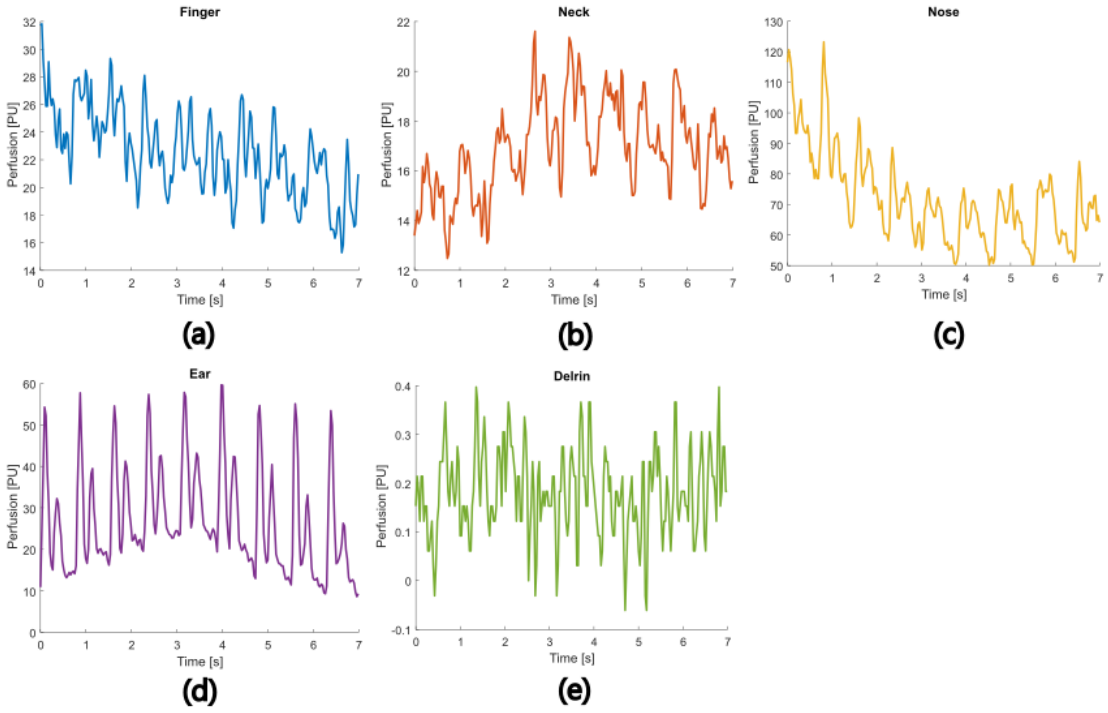

FIGURE 18: The first seven seconds for each of the individual LDPM measurements. (a) finger, (b) neck, (c) nose, (d) ear, (e) Delrin plate.

4.2.2 120 second measurement

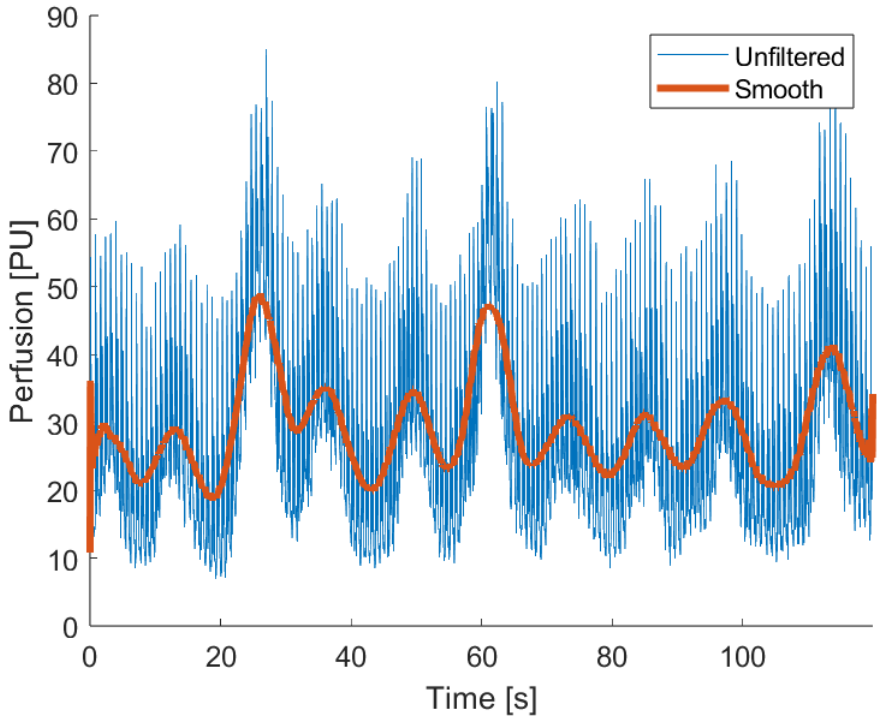

FIGURE 19: A full two-minute LDPM measurement on the ear with a smoothing function with a span of 0.05 applied.

Figure 19 shows a full two minute measurement with a MatLab *smooth* filter applied (span of 0.05). Looking at a longer time period, several different waves are visible. The first is the cardiac cycle with a period of about 1 second. Secondly, the breathing pattern with a period of about 10 seconds. Finally, the deeper breaths, which occur about every 30 seconds. These deep breaths temporarily increase blood flow by a factor of two.

4.3 In vivo SDF measurements

Sidestream dark field microscopy was used to visualise the microcirculation in the skin. The papillary loops and superficial plexus are clearly visible. See Figure 20. The right image shows a processed image with a *hot* colormap. The range has been set quite narrow, to improve the contrast. The RBCs can be seen moving in single file through the smallest capillaries.

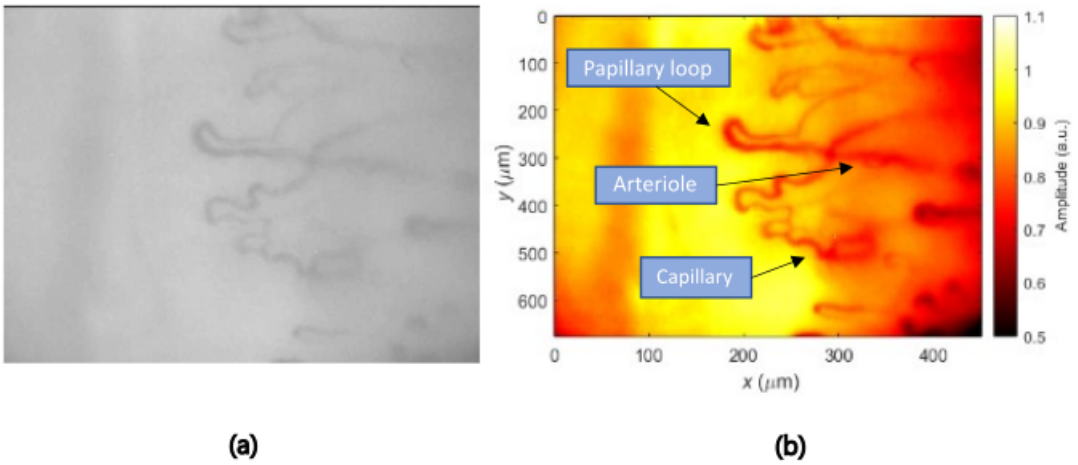

FIGURE 20: (a) A raw SDF image of the finger, as seen during the measurements. Magnification 10× (b) The same SDF image after being processed with a narrow color bar.

5 Phantoms: Materials and methods

5.1 Materials

5.1.1 Structure of the phantoms

The phantom has been obtained in cooperation with A. Rezaei from Physics of Fluids, University of Twente. The basis of the phantom, shown in figure 21, is the ring-shaped PDMS holder. It has an outer diameter of approximately 35 mm and an inner diameter of 20 mm. The thickness is 10 mm. There are several small holes through the side of the ring where a needle can be placed. These holes are 0.45 mm in diameter. This object was designed using 3D software. It was then 3D printed using a resin 3D printer. After printing, two luer lock needles are inserted into opposite holes in the sides. A thin fishing wire of 60 or 100 µm (Shakespeare TeamMatch K2) is placed through these needles. A PDMS mix is then prepared. This is made by combining Sylgard 184 silicone elastomer base and hardener in a 10:1 ratio. It was then poured into the ring, covering the wire and needles, and cured in an oven at 80°C for three hours. Once the PDMS had cured, the fishing wire was removed, leaving a channel.

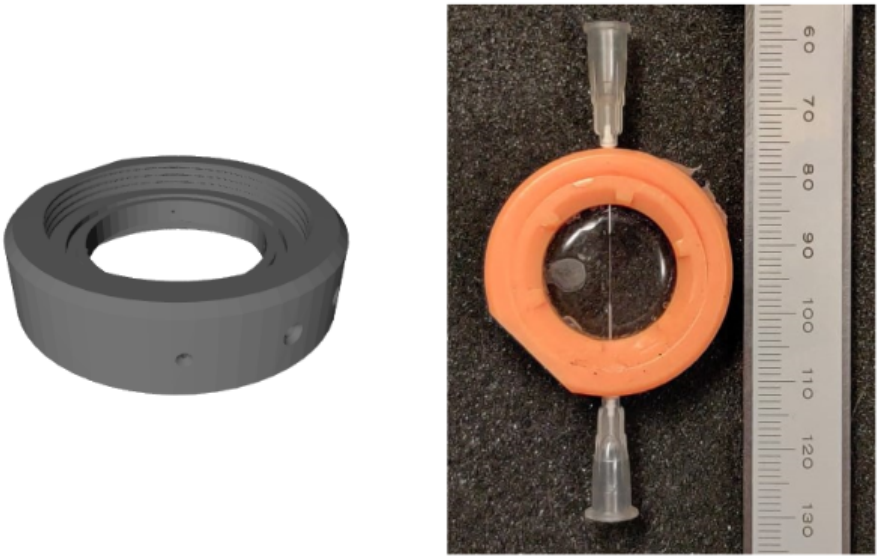

FIGURE 21: One of the 100 μm phantoms. Designed by Ali Rezaie in the Physics of Fluids group, University of Twente. (a) shows a 3D model of the inner ring. (b) shows a finished phantom.

5.1.2 Setup

To reach this channel from outside of the ring, several components connect the channel to a syringe pump. A picture of the setup can be seen in figure 22. A schematic view can be seen in figure 23.

The fluid is moved by two syringes. These syringes are connected to each other by a system of tubes, connectors and the phantom. First, the syringe needle is covered by a sleeve. This sleeve is connected to a piece of HPFA tubing via a set of adapters. The HPFA tubing

is connected to the luer lock needle via an adapter. The luer lock needles are connected directly to the PDMS in the phantom.

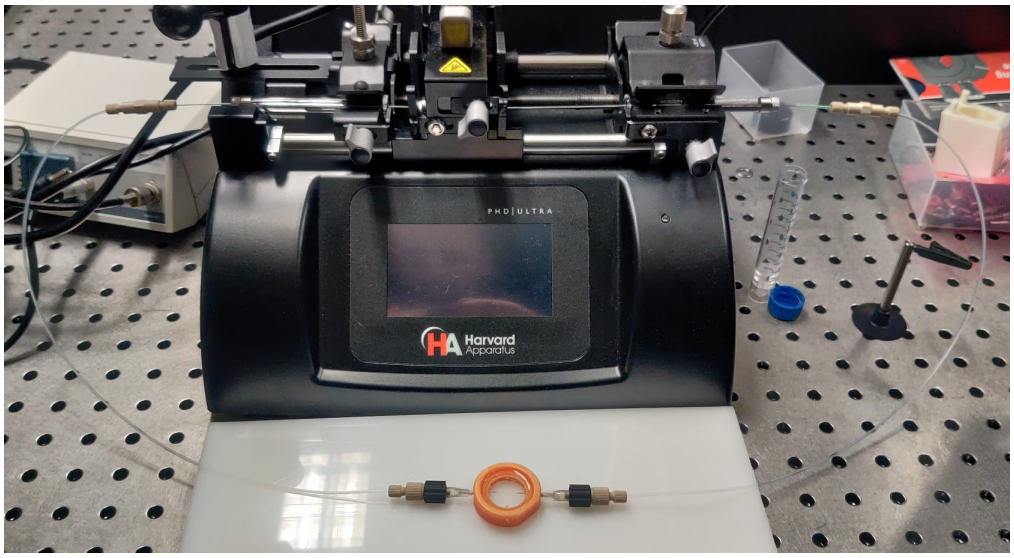

FIGURE 22: A picture of the whole flow setup.

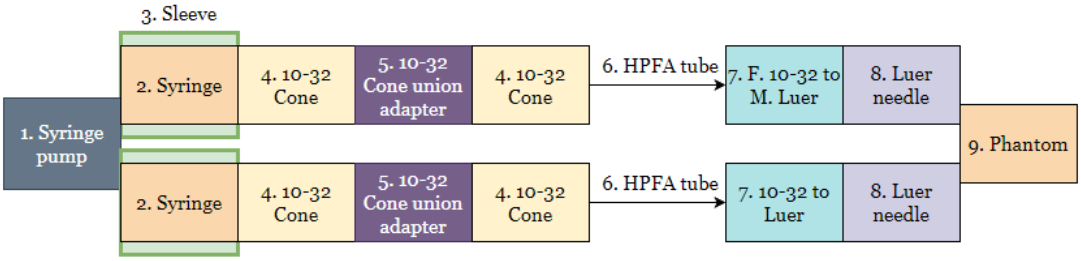

FIGURE 23: A flowchart that shows all different components of the setup. The specifications can be found in table 4

Number	Specifications	Diameters
1	Hard systems PHD syringe pump	-
2	Hamilton syringe 25µL 80230	0.718mm OD x 0.413mm ID x 2" Len
3	IDEX F-242X Nanotight tubing	1/16" OD x 0.0155 ID x 1.55 Len
4	IDEX Nanotight fitting	1/16" OD
5	IDEX Product SKU: CIL-P-779-01	125µm ID
6	IDEX 1907L High Purity Plus PFA	1/16" OD x 0.02" ID
7	IDEX Product SKU: CIL-P-656	0.050" ID
8	Luer lock needle 27Ga and 23Ga	210µm and 340µm ID
9	Microchannel Phantom	100 and 60 µm ID

TABLE 4: The components of the flow phantom measurements.

5.1.3 Preparing blood

Water will be used for the initial flow through the phantoms. Once this has been proven to work, blood will be used. This will allow comparisons to be made with in vivo measurements.

Before the blood is collected, a 1 litre container is prepared with 6 mL of 0.9 % glucose, 3 mL of Heparin-Natrium, 1.8 mL of 50 % glucose. This was done in collaboration with the blood lab of the University of Twente, under supervision of A.F. Costa Martins of Engineering Organ Support Technologies (EOST). Without these additives, the blood would clot quickly on a foreign surface such as a container. After receiving the blood, the container was placed on a Fisherbrand Open Air Rocker to further prevent clotting. To ensure that fresh blood was used in the measurements, the experiments were carried out on the same day that the blood was received.

Before taking the flow measurements, 3 mL of blood is transferred into a small cylinder. This is done to control the damage if the cylinder is knocked over.

5.2 Methods

5.2.1 Microscopy

A total of four phantoms were obtained. There were two pairs of phantoms with the same diameter. To ensure that the phantoms had the correct shape and diameter, bright field microscopy was performed. This was done with the help of J.R.M. Plass, (Developmental BioEngineering, University of Twente), laboratory ZH168(?).
To make sure that the channels were completely hollow and without cracks, fluorescence microscopy was performed on one of the phantoms. By placing a few drops of green fluorescent protein (FITC-Dextran, 4 kDa, 1 mg/ml in water, GFP 1%) on one of the needles, the fluid will make its way through the channel by capillary action. This was done with the help of dr.ir. K.M. Pondman (Developmental BioEngineering, University of Twente).

5.2.2 Flow measurements

The first goal is to observe a flow in the channel. To do this, the left needle is placed in the phantom. The other needle is placed in a smaller container filled with blood. The syringe pump is set to a withdrawing mode, to draw the blood into the needle. Once the 25 µL of blood has been drawn up, the needle is placed into the phantom. The pump is then set to infuse mode to push out the blood that has just been drawn in. The flow rate is set to 10 µL/min.

SDF First, a drop of ultrasound gel is placed on the phantom surface. This is done to reduce image artefacts caused by the change between media. The SDF probe is placed perpendicular to the channel. See figure 24 (a). First, a sharp image is generated by finding the optimum magnification and illumination level of the probe.

Once this is done, the flow measurements are started. During these measurements, the AVA software is used to make videos of the flow through the channel. These videos are used to analyse the flow pattern and flow velocity.

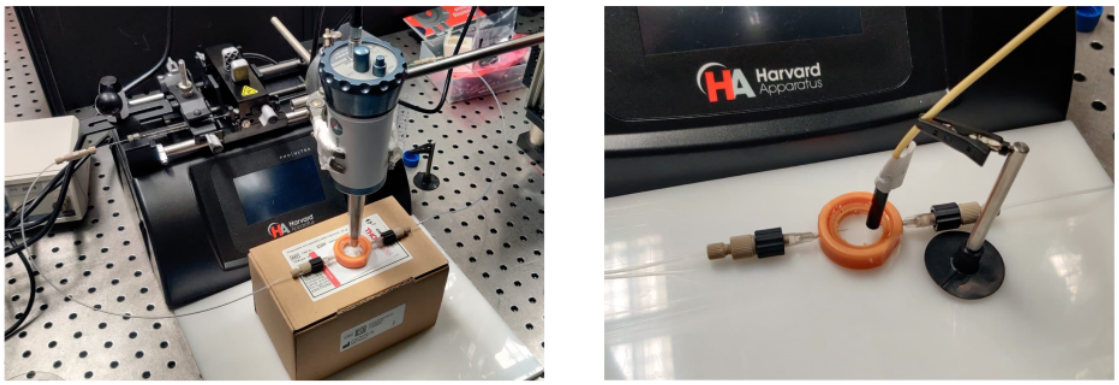

(a) (b)

FIGURE 24: (a) The SDF probe, placed on the channel. (b) the LDPM probe, positioned perpendicular to the channel

LDPM As with SDF, the LDPM probe is placed in a drop of ultrasound gel. It is held in place by a small holder. This ensures that it remains in one position during the measurements. Due to the large fibre separation compared to the channel diameter, it takes some time to place the probe correctly over the channel. When the correct position is found, the flow measurements are started. The Perisoft software is running throughout the measurement.

6 Phantoms: Results

6.1 Microscopy

Bright-field microscopy
Figure 25 shows the results of bright field microscopy. The scale bar in the image can be used to measure the inner diameter of the channel. It is 100 µm for phantoms (a) and (c) and 60 µm for phantoms (b) and (d).

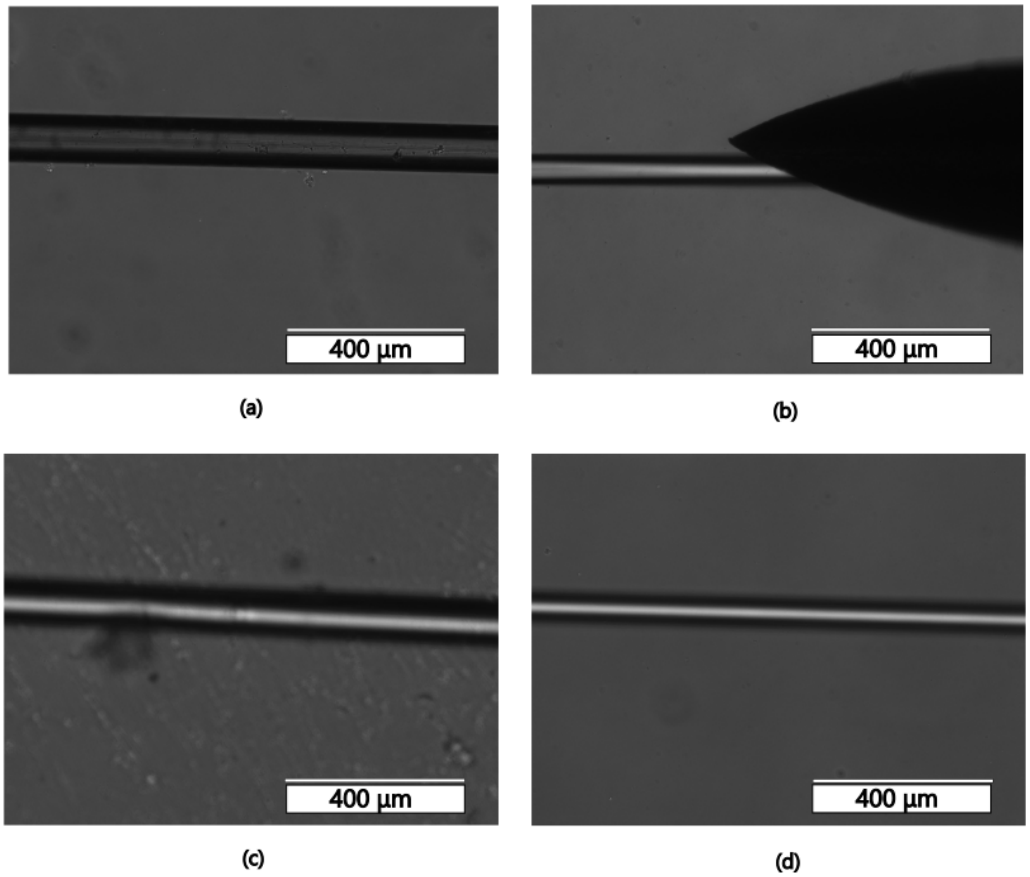

FIGURE 25: (a) & (c) bright-field microscopic images of the 100 µm phantoms. Magnification: 10×. (b) & (d) bright-field microscopic images of the 60 µm phantoms. Magnification: 10×. In (b), part of the Luer Lock needle is visible.

Fluorescence microscopy
Figure 26 shows the fluorescence microscopy image. The GFP has made its way through the channel. No irregularities were visible in the field of view of the microscope.

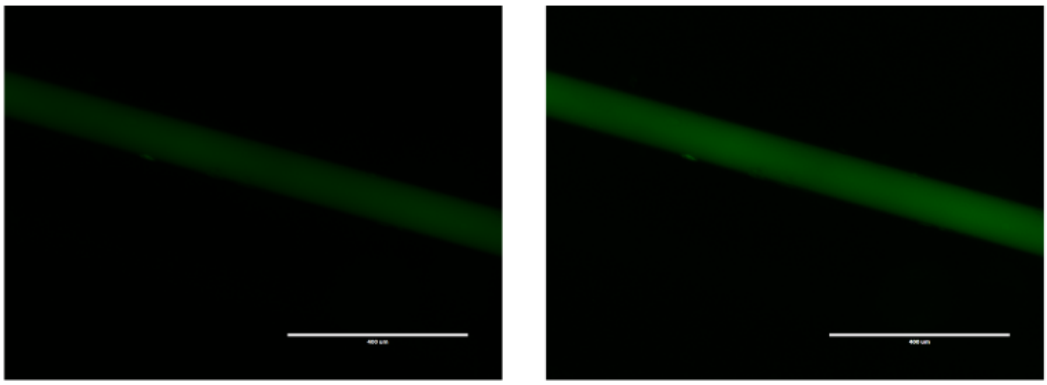

FIGURE 26: (a) & (b) Phantom 1 (ID: 100 µm) after Green Fluorescent Protein is inserted from the side. Magnification: 10×. The scalebar shows a distance of 400 µm. (b) shows the same image, but with the brightness increased.

6.2 SDF analysis

6.2.1 Image quality

The 60µm channel phantoms could not produce a clear image. See figure 27. There are several reasons for this. The first reason is that these phantoms had a slightly thicker PDMS layer. The SDF microscopy has a measurement depth of a few hundred micrometer. The second reason is that the PDMS layer is not completely flat. Therefore it's impossible to position the SDF probe flat on the phantom. It was therefore decided to proceed with the 100 µm channels only.

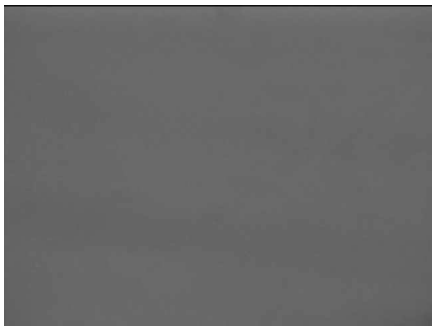

FIGURE 27: A frame of an SDF video of the 60 µm channel.

6.2.2 Flow realisation

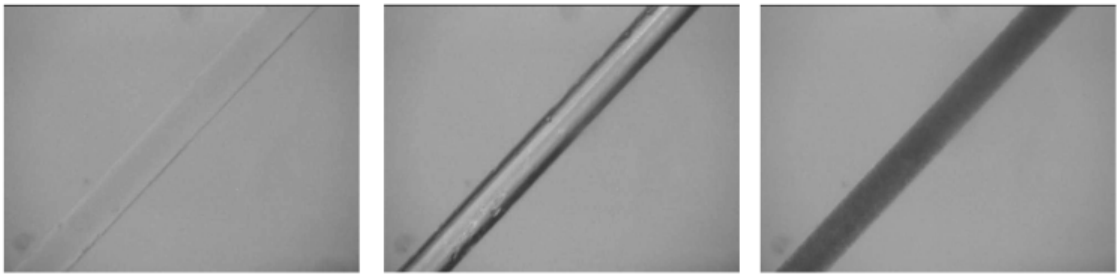

FIGURE 28: (a) shows the channel when it is filled with water. (b) is the channel filled with air. (c) is the channel filled with blood.

Using a flow rate of 10 µl/min, it was possible to observe a consistent flow. By using the MatLab script, the contrast of the video can be improved.

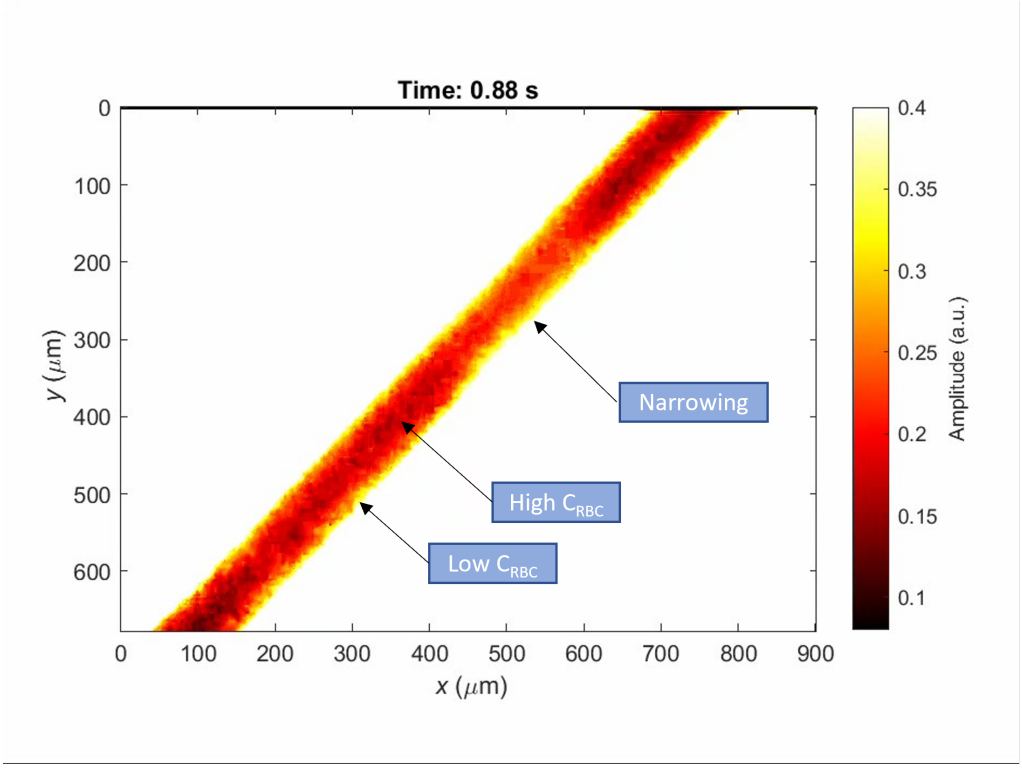

FIGURE 29: A frame of a processed SDF video. The measurement was done on the 100 µm channel. See video 10.6

Looking at the contrast-enhanced video (see video 10.6), there is a laminar flow visible. The amplitude is lower in the centre. This means that the concentration of RBCs is higher. At the edges of the channel, there's almost no RBCs. There also appears to be a small constriction in the channel.

6.2.3 Velocity inside the channel

Theoretical velocity
A flow through the channel has been achieved in the 100 µm diameter channel. First, the relationship between the set flow rate value and the measured flow rate is established. The analysis is performed using an SDF video of blood flowing through the channel.

The flow rate has been set to 10μl/min. This corresponds to $16.67 \cdot 10^{-11}$ m^3/s
The cross-section of the channel is $A = \pi \cdot (\frac{100 \cdot 10^{-6}}{2})^2 = 7.85 \cdot 10^{-9}$ m^2. This leads to a velocity of:

$$V = \frac{Q}{A} = \frac{16.67 \cdot 10^{-11}}{7.85 \cdot 10^{-6}} = 2.12 \text{ cm/s} \tag{8}$$

Observed velocity
A MatLab script is used to measure the actual velocity of the blood in the channel. The velocity is measured by selecting an air bubble in two different frames (time points). A MatLab script calculates the distance between these points. By dividing this distance by the time between the frames, the velocity is calculated. Looking at the video, it is clear that the velocity of the air bubbles (and therefore the fluid) changes a lot during the measurement. Therefore, the velocity of five different bubbles is measured. The result is as follows:

Air bubble [#]	Frame 1 [n]	Frame 2 [n]	Velocity [mm/s]
1	1	79	0.21
2	197	374	0.13
3	1050	1176	0.18
4	1459	1565	0.21
5	1754	1884	0.17
6	2155	2255	0.22
7	2616	2775	0.13
8	2940	3064	0.18
9	3290	3381	0.24
10	3475	3554	0.28
11	3690	3768	0.28
12	3868	3925	0.37
Mean ± SD	-	-	0.22 ± 0.07

TABLE 5: The velocity of the air bubbles, as measured the recording of the SDF measurement.

This measured velocity is around 100 times slower than theoretical velocity.

6.3 LDPM measurement

The LDPM measurement, see figure 30, consists of several steps. The first 170 seconds are when the syringe pump is turned on. During this time the signal remains constant at 0. 170 seconds after the start of the measurement, the left needle is loosened slightly. The high peak in the signal (at 170 seconds) corresponds to the movement of the needle. This

releases the pressure in the system, causing the blood to move very quickly through the channel. This continues for at least 300 seconds. After 470 seconds, the needle is removed completely. After this, the signal hovers around a value of about 1.5.

This method of producing flow has also been observed through SDF microscopy. It is observed that when the needle is loosened slightly, the blood starts flowing very quickly. When the needle is removed completely, the blood is stationary inside the channel. This matches the data measured through LDPM.

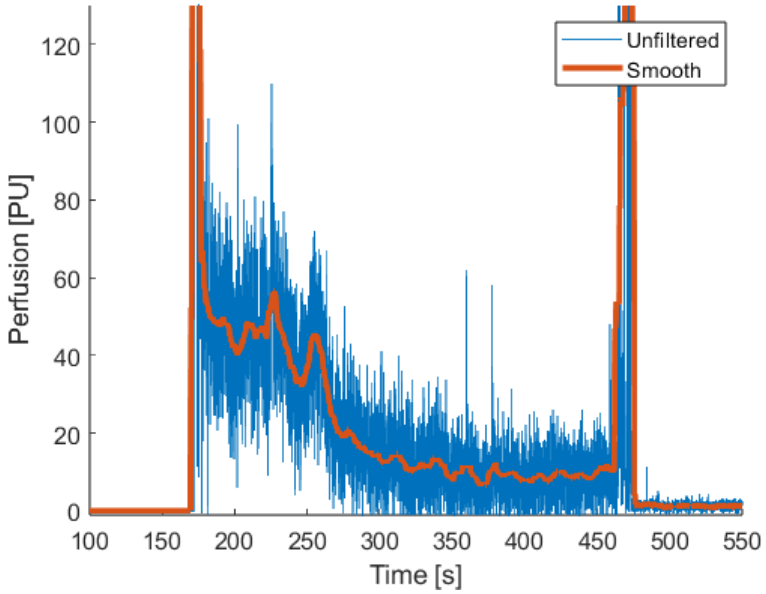

FIGURE 30: The measured perfusion over time during the LDPM measurement on the phantom.

7 Discussion

7.1 In Vivo LDPI measurements

Measurement results With these measurements (see figure 14), we have shown the local difference in LDPI signal on the human skin. Each of the four different spots showed a different perfusion, intensity and cardiac pattern. These differences can be attributed to local differences in the anatomy of the microcirculation. No big artefacts are visible in the measurements.
Some slight fluctuations are visible in the intensity graphs. This originates from the shot noise, dark shot noise and readout noise.
The change in perfusion value is visible in the power spectra.

LDPI ROI selection The perfusion signal is very dependent on the region of interest selected. After each measurement, the region of interest has been selected manually. While this allows for more options, it is not always known what position and size of the ROI produces the clearest signal.

Laser During in vivo LDPI measurements, the laser was unreliable. Sometimes, The power spectrum showed high peaks around 4kHz, 8kHz and 12kHz. When this occurred, the measurements contained much more noise.
These peaks could be a result of mode hopping. These peaks varied in width from points to 2 kHz wide peaks. A possible cause could be temperature drift. To prevent this, two small fans were placed on the laser's heat sink. These helped to resolve the problem for the most part. Eventually, it was noted that the peaks disappeared when turning the laser off and on again. By carefully timing this, measurements could be performed without problems.

7.2 In Vivo LDPM measurements

Measurement results With these measurements, we have shown the local difference in LDPI signal on the human skin. Each of the four different spots showed a different perfusion value and cardiac pattern.

Noise artefacts Because the probe was connected to the skin with strong double-sided tape, there was consistent contact. The LDPM measurements still showed considerably more noise than the LDPI measurements. This originates from movement of the optical fibre. When the fibre is even slightly moved, the interference pattern of the light changes. These artefacts can be prevented by keeping the fibre in the same position for the whole measurement.

7.3 In Vivo SDF

Measurement results Bringing the blood vessels into focus proved to be quite difficult. This is because the depth of focus of the optical system is limited to a few hundred microns. The Microscan device would work better in areas with a thinner layer of dermis, such as under the tongue.

7.4 Phantoms

Microscopy By making brightfield microscopy images, the inner diameter could be confirmed. Another observation from the microscopy images is the clarity of the PDMS. Although all PDMS media contain the same ingredients, they do not look exactly the same in the images. This is probably due to a slightly different depth of focus or fingerprints on the PDMS.

Fluorescence microscopy showed that the channel was completely hollow. This method requires very little effort and produces a clear visualisation. This technique could be particularly useful when moving on to more channels or complex shapes.

Coupling issues Because of the pressure differences, only a completely airtight setup could produce flow in the setup. Any small gap, such as an adapter not being tight enough, meant no flow. Flow was also possible when one of the needles was removed. When you remove the needle, you create a local drop in pressure. When the blood was about twenty-four hours old, this became the only way to produce flow.

SDF results The measured velocity of 0.2 mm/s in the channel was 100 times slower than the theoretical velocity. This means that the setup was not working fully as intended.

The flow looked laminar. By calculating Reynold's number, we can see if the flow is truly laminar.

$$Re = \frac{\rho V D}{\mu} = \frac{994 \cdot 0.2 \cdot 10^{-3} \cdot 100 \cdot 10^{-6}}{4.5} = 4.56 \tag{9}$$

where Re is a dimensionless number, ρ is the density in kg/m3, V is the velocity of the moving fluid in m/s, d is the tube diameter in m and μ is the dynamic viscosity in mPa $\cdot$ s.

The formula shows a Reynold's number of 4.56. Flows with a Reynold's number below 2900 can be considered laminar flow. This confirms that the observation we made was correct.

LDF results Only LDPM was performed on the phantoms. There was no lens available strong enough to measure an LDPI signal on 100 µm.
During this research, we were able to perform an LDPM measurement on the microchannel. However, it was not possible to generate a signal while the syringe pump was pumping. The measured signal was obtained by slightly loosening one of the needles, which created a flow. This flow was maintained for at least 300 seconds. Judging by the intensity of the signal, this flow slowly decreased over time. The intensity value starts at about 50 PU and drops to about 10 PU during the measurement. Due to the imprecise nature of this measurement, no comparison can be made between this signal and the in vivo measurements.

LDPM probe positioning With a fibre seperation of 250µm, positioning the LDPM probe correctly on the 100µm channel is a challenge. During the measurements, the probe was moved around until it produced a signal. However, it was almost impossible to know whether the probe was directly over the channel or only partially over it.

Biological zero problem During the LDPM measurement, there most likely was no flow after the needle had been removed. There was still some noise in the signal. According to Kernick et al [15], this signal is due to Brownian motion of larger molecules in the blood.

Blood Even though the blood was prepared with heparin to prevent clotting, it still became noticeably thicker after about twelve hours. This meant that there was a very narrow window in which to make the measurements. Twenty-four hours or more after receiving the blood, it was impossible to draw blood through the needles. One option to solve this would have been to dilute the blood. This would reduce the viscosity but still produce a signal. Due to time constraints, this has not been attempted.

7.5 Alternative Microchannel: Glass microneedle

While brainstorming different ways to make a channel in the micrometer range, multiple options were considered. One of these options was to use a glass pipette puller. This was done with the help of A. Kocer (Bioelectric Signaling and Engineering, University of Twente).

Methods

A Sutter P-1000 micropipette puller was used. Small glass cylinders (ID: 1 mm) were placed in this device. The device has several inputs. Heat, pull, velocity, time and pressure. These parameters are dimensionless numbers between 0 and 255. These values together determine the speed and force with which the glass is pulled. The ideal temperature (Heat) must be measured using a ramp test. The heating filament is increased until the glass tube breaks. To perform a stretching test, a glass tube is carefully inserted into the machine. The centre of the tube should be aligned with the platinum heating element. When the start button is pressed, the heating elements begin to glow white hot. The tube is then pulled apart (stretched) until it breaks. This break creates a needle tip. In this experiment, six runs were made with different parameters to try to make the tip as thin as possible.

Results

Figure 31 (a) shows two pairs of microneedles, made with this device. Figure 31 (b) shows a bright field microscopy image. The whole needle is not visible in the image, so the minimum diameter is not known exactly. Using the scale in the image, it is at most 5 µm. Due to time constraints, it was decided not to continue with this technique.

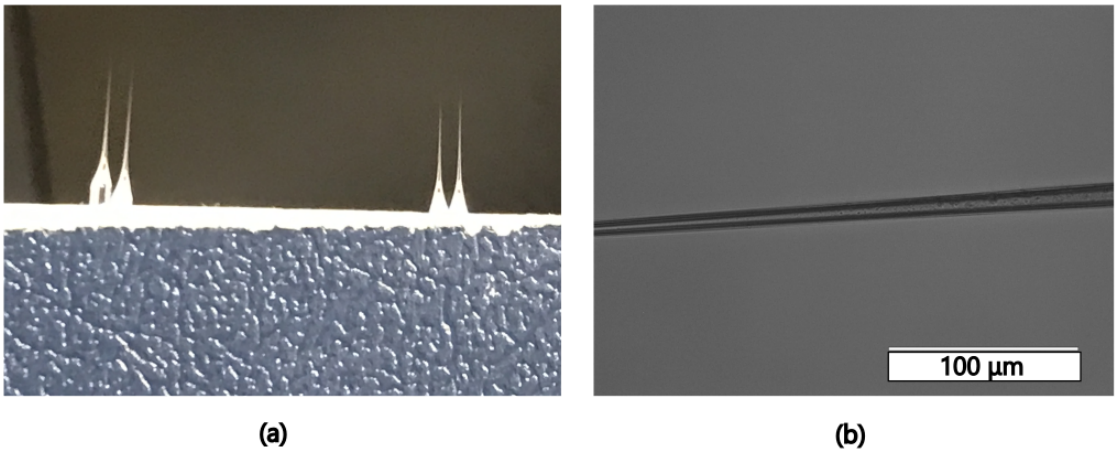

FIGURE 31: (a) Two pairs of produced microneedles. (b) Brightfield microscopic image of one of the needles. Magnification 40×

8 Conclusion

This research has taken a first step towards understanding the composition of laser Doppler flowmetry signals. In vivo LDF measurements were performed to gain experience with the system and to observe differences in the signal. Each different site on the body showed a different cardiac pattern in the perfusion signal. SDF was used to visualise the microcirculation of blood within the skin.
As a first step in simulating the microcirculation, phantoms were made with a 100 µm diameter channel. In this channel, a visible but non-uniform blood flow was realised. An LDPM measurement was performed on this blood flow. Although a signal was obtained, no relationship between flow rate and perfusion could be established. In order to compare the in vitro and in vivo measurements, systematic measurements should be carried out where the flow rate in the channel can be both controlled and optically measured.

9 Future work

During this research, some problems and difficulties were encountered. For future research on this topic, I recommend possible changes and improvements.

Phantom design While the phantom used in this research had a very small diameter channel, the other components were not comparable to a real blood vessel. To make it more similar to the in vivo situation, some changes could be made. Scattering particles could be added to the PDMS medium. This would make it more like human skin, rather than a completely transparent medium. Another change could be to change the material of the medium. Although PDMS is easy to work with, it does not mimic the flexible nature of a blood vessel. Possible media include agarose gel and flexible polymers. Finally, this research has only used a single 100 µm channel. In real skin, there are usually at least 60 capillaries per square millimetre [16]. These capillaries also vary in shape and depth. Therefore, when designing a new phantom, it should be attempted to place multiple channels at multiple depths.

Setup To measure an LDF signal on the phantom, a transmission setup may work better. This is because the laser and detection fibres are next to each other, making positioning difficult. Having these fibres on the same optical axis would make positioning easier.

Another priority should be to reduce the number of adapters and converters. If a problem occurs during the measurement, such as the fluid not moving, it takes a long time to find out where the problem is.
A device called the Flow EZ is specifically designed to pump fluids very slowly. It uses a reservoir to store the fluid and uses air pressure to push the fluid out. It can also be easily attached to a Luer lock. Using this device would remove a lot of complexity from the setup. The only problem with this setup would be that it would be more difficult to create a closed loop system. To make this work, two pumps would be needed to pump in opposite directions at the same time. A schematic view of the setup can be seen in figure 32.

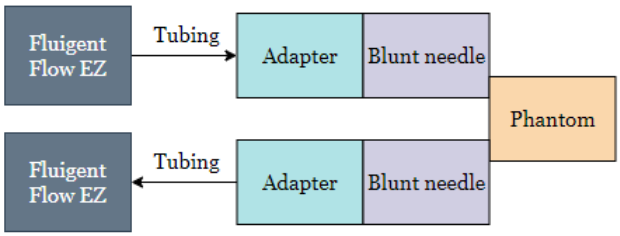

FIGURE 32: Schematic illustration of a simpler setup by using a Fluigent Flow EZ instead of syringe pump.

Another problem with the setup was the fragile connection between the luer lock needle and the PDMS of the phantom. To get the blood into the setup, the needle had to be removed and reinserted. After doing this several times, the thin layer between the needle channel hole and the phantom was pierced. This created a leak in the system and rendered the phantom unusable. An improvement might be to use blunt needles instead of the sharp ones. Another option would be to disconnect another component in the setup.

Phantom LDPM One of the things that failed was measuring the LDPM signal at different flow rates. Ideally, we would take a measurement for one minute and increase the flow rate every ten seconds. The result could be a graph with a step-like function, as in the figure 33.

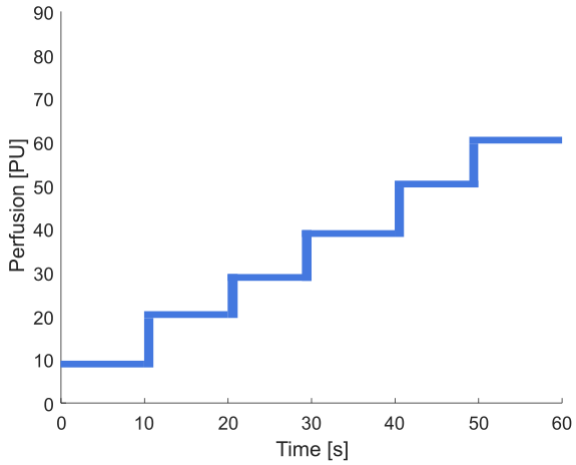

FIGURE 33: An ideal LDPM measurement where the blood flow is increased stepwise every ten seconds.

References

[1] P Goedhart, M Khalilzada, Rick Bezemer, Can Ince, and Can Ince. Sidestream dark field (sdf) imaging: A novel stroboscopic led ring-based imaging modality for clinical assessment of the microcirculation. *Optics express*, 15:15101–14, 12 2007.

[2] Christian Zakian and Mark Dickinson. Laser doppler imaging through tissues phantoms by using self-mixing interferometry with a laser diode. *Opt. Lett.*, 32(19):2798–2800, Oct 2007.

[3] Hanna Jonasson, Ingemar Fredriksson, Marcus Larsson, and Tomas Strömberg. Validation of speed-resolved laser Doppler perfusion in a multimodal optical system using a blood-flow phantom. *Journal of Biomedical Optics*, 24(9):095002, 2019.

[4] S. M. Shams Kazmi, Ehssan Faraji, Mitchell A. Davis, Yu-Yen Huang, Xiaojing J. Zhang, and Andrew K. Dunn. Flux or speed? examining speckle contrast imaging of vascular flows. *Biomed. Opt. Express*, 6(7):2588–2608, Jul 2015.

[5] Vinayakrishnan Rajan, Babu Varghese, Ton van Leeuwen, and Wiendelt Steenbergen. Review of methodological developments in laser doppler flowmetry. *Lasers in medical science*, 24:269–83, 02 2008.

[6] Wiendelt Steenbergen. dynamic speckles 1, bmo lecture, university of twente, 2017.

[7] Beat frequencies. `http://hyperphysics.phy-astr.gsu.edu/hbase/Sound/beat.html#c1`. Accessed: 2023-04-28.

[8] Ingemar Fredriksson, Carina Fors, and Johannes Johansson. Laser doppler flowmetry – a theoretical framework. 01 2012.

[9] Ingemar Fredriksson, Marcus Larsson, and Tomas Strömberg. Measurement depth and volume in laser doppler flowmetry. *Microvascular Research*, 78(1):4–13, 2009.

[10] Jean-Luc Cracowski and Matthieu Roustit. Human skin microcirculation. *Comprehensive Physiology*, 10:1105–1154, 07 2020.

[11] Skin and skin appendage. `https://www.amboss.com/us/knowledge/Skin_and_skin_appendage`. Accessed: 2023-04-28.

[12] Elaine Nicpon Marieb and Katja Hoehn. *Human anatomy & physiology.* Pearson, Hoboken, New Jersey, eleventh edition edition, 2018.

[13] Curt M. Treu, Omar Lupi, Daniel A. Bottino, and Eliete Bouskela. Sidestream dark field imaging: The evolution of real-time visualization of cutaneous microcirculation and its potential application in dermatology. *Archives of Dermatological Research*, 303(2):69–78, Oct 2010.

[14] perimed.instruments.com. Laser doppler probes, Dec 2012.

[15] D. P. Kernick, J. E. Tooke, and A. C. Shore. The biological zero signal in laser doppler fluximetry - origins and practical implications. *Pflugers Archiv European Journal of Physiology*, 437(4):624–631, 1999.

[16] Haythem Debbabi, Laurent Uzan, Jean Jacques Mourad, Michel Safar, Bernard I. Levy, and Eduardo Tibiriçà. Increased Skin Capillary Density in Treated Essential Hypertensive Patients*. *American Journal of Hypertension*, 19(5):477–483, 05 2006.

10 Appendix

10.1 Video 1: Finger LDPI measurement

https://figshare.com/s/0b50b5563f7ac999fb1e (clickable)

10.2 Video 2: Neck LDPI measurement

https://figshare.com/s/e902677d4e8e92daad36 (clickable)

10.3 Video 3: Nose LDPI measurement

https://figshare.com/s/83dbc06888d35e7bb2fc (clickable)

10.4 Video 4: Ear LDPI measurement

https://figshare.com/s/b81100a5a6898e57d72c (clickable)

10.5 Video 5: Delrin LDPI measurement

https://figshare.com/s/b43285c6beca46198611 (clickable)

10.6 Video 6: Processed SDF video

https://figshare.com/s/a23c99339735be0305b9 (clickable)

11 Acknowledgements

For their contribution to this research, I want to thank the following people:

Biomedical Photonic Imaging: Ata Chizari, Tom Knop and all the students
Developmental BioEngineering: Irene Konings, Kirsten Pondman
Physics Of Fluids: Guillaume Lajaunie, Ali Rezaie
Engineering Organ Support Technologies: Ana Martins Costa
Bioelectric Signaling and Engineering: Armagan Kocer